Transcription Factor Stat5 Synergizes with Androgen Receptor in Prostate Cancer Cells

Shyh-Han Tan,[1] Ayush Dagvadorj,[1] Feng Shen,[1] Lei Gu,[1] Zhiyong Liao,[1] Junaid Abdulghani,[1] Ying Zhang,[2] Edward P. Gelmann,[3] Tobias Zellweger,[4] Zoran Culig,[6] Tapio Visakorpi,[7] Lukas Bubendorf,[5] Robert A. Kirken,[8] James Karras,[9] and Marja T. Nevalainen[1]

[1]Department of Cancer Biology, Kimmel Cancer Center, Thomas Jefferson University, Philadelphia, Pennsylvania; [2]Biostatistics Unit and [3]Department of Oncology, Lombardi Comprehensive Cancer Center, Georgetown University, Washington, District of Columbia; [4]St. Clara Hospital; [5]Institute for Pathology, Basel, Switzerland; [6]Department of Urology, University of Innsbruck, Innsbruck, Austria; [7]Institute of Medical Technology, University of Tampere and Tampere University Hospital, Tampere, Finland; [8]Department of Biological Sciences, University of Texas, El Paso, Texas; and [9]ISIS Pharmaceuticals, Carlsbad, California

Abstract

The molecular mechanisms underlying progression of prostate cancer to the hormone-independent state are poorly understood. Signal transducer and activator of transcription 5a and 5b (Stat5a/b) is critical for the viability of human prostate cancer cells. We have previously shown that Stat5a/b is constitutively active in high-grade human prostate cancer, but not in normal prostate epithelium. Furthermore, activation of Stat5a/b in primary human prostate cancer predicted early disease recurrence. We show here that transcription factor Stat5a/b is active in 95% of clinical hormone-refractory human prostate cancers. We show for the first time that Stat5a/b synergizes with androgen receptor (AR) in prostate cancer cells. Specifically, active Stat5a/b increases transcriptional activity of AR, and AR, in turn, increases transcriptional activity of Stat5a/b. Liganded AR and active Stat5a/b physically interact in prostate cancer cells and, importantly, enhance nuclear localization of each other. The work presented here provides the first evidence of synergy between AR and the prolactin signaling protein Stat5a/b in human prostate cancer cells. [Cancer Res 2008;68(1):236–48]

Introduction

Identification of molecular changes that lead to androgen-independent growth of prostate cancer cells is critical for the development of better therapeutic interventions for primary and advanced prostate cancer. Hormone-refractory prostate cancer is characterized by continued expression of androgen receptor (AR) and androgen-regulated genes, suggesting that the AR signaling pathway remains active despite low levels of circulatory androgens (1). AR is a cytoplasmic protein which, upon ligand binding, undergoes conformational changes, which leads to translocation of the AR to the nucleus. In the nucleus, AR undergoes intramolecular interactions that regulate its subsequent interactions with coactivators and influence its activity (2). Ligand-bound activated AR binds to specific DNA sequences at promoter regions of androgen-responsive genes to initiate transcription (3).

Adaptation of prostate cancer cells to androgen deprivation is known to involve several different molecular mechanisms. First, the AR gene is amplified in ~25% to 30% of patients who experience disease recurrence (4). Second, somatic mutations of the AR in hormone-refractory prostate cancer result in receptors with elevated affinity for steroid hormones other than androgens and for pharmaceutical antiandrogens (5). In addition, mutations of the AR affect coactivator and corepressor binding (6). Third, protein kinase signaling pathways may promote proliferation and survival of prostate cancer cells directly or through stimulation of the AR in hormone-refractory prostate cancer.

One such protein kinase signaling pathway that may promote androgen-independent growth of prostate cancer via interaction with AR is the Janus-activated kinase (Jak2)–signal transducer and activator of transcription 5 (Stat5) signaling cascade. Stat5 belongs to the seven-member Stat gene family of transcription factors (7). There are two highly homologous isoforms of Stat5, 94-kDa Stat5a and 92-kDa Stat5b, which are encoded by separate genes (7). Stat5a and Stat5b (hereafter called Stat5a/b) are latent cytoplasmic proteins that act as both cytoplasmic signaling proteins and nuclear transcription factors. Stat5a/b becomes active by phosphorylation of a specific tyrosine residue in the carboxy-terminal domain (7) by a tyrosine kinase typically of the Jak protein family (8, 9). After phosphorylation, Stat5a and Stat5b homodimerize or heterodimerize and translocate to the nucleus, where they bind to specific Stat5a/b response elements of target gene promoters (7).

Stat5a and Stat5b are the principal signaling proteins that mediate the effects of prolactin (Prl) in normal and malignant prostate cells (10–12). Prl is a mitogen and survival factor for prostate cells (13–15), and transgenic mice overexpressing the Prl gene develop massive hyperplasia of prostate (16–18). Correspondingly, Prl-null mice have smaller prostates than their wild-type (WT) counterparts (19). Prl protein and its receptor are expressed in malignant prostate epithelium (12, 13, 20, 21), and Prl protein expression in human prostate cancer is associated with high histologic grade (12). In line with these findings, transcription factors Stat5a and Stat5b are highly critical for the viability of human prostate cancer cells (22). This was later confirmed in the TRAMP mouse prostate cancer model (23). Prostate acinar epithelium is defective in Stat5a knockout mice (10), and Stat5a/b is constitutively active in human prostate cancer (12, 22, 24). Similar to autocrine Prl, expression of active Stat5a/b associates with high histologic grade of human prostate cancer (n = 114, P < 0.0001; ref. 12), a finding that we later confirmed in a larger, independent set of human prostate cancer specimens (n = 357,

Note: Supplementary data for this article are available at Cancer Research Online (http://cancerres.aacrjournals.org/).

Requests for reprints: Marja T. Nevalainen, Department of Cancer Biology, Kimmel Cancer Center, Thomas Jefferson University, 233 S. 10th Street, BLSB 309, Philadelphia, 19107 PA. Phone: 215-503-9250; Fax: 215-503-9245; E-mail: marja.nevalainen@jefferson.edu and M_Nevalainen@mail.jci.tju.edu.

doi:10.1158/0008-5472.CAN-07-2972

$P = 0.03$; ref. 24). Importantly, we also showed that active Stat5a/b in primary prostate cancer predicts early disease recurrence (24). These findings led us to propose that Stat5a/b may promote androgen-independent growth of prostate cancer. In this study, we hypothesized that Stat5a/b interacts with AR in prostate cancer cells.

Here, we show that Stat5a/b is in the active state in the majority of hormone-refractory clinical human prostate cancers. We further show that the active Stat5a/b signaling pathway increases transcriptional activity of AR in prostate cancer cells. Ligand-bound AR, in turn, increases transcriptional activity of Stat5a/b. The functional synergism of Stat5a/b and AR in prostate cancer cells involves direct physical interaction between the two. Liganded AR enhances nuclear localization of Stat5a/b, and active Stat5 promotes nuclear translocation of AR. In summary, this work establishes the novel concept that Stat5a/b interacts with AR signaling in human prostate cancer cells.

Materials and Methods

Primary human prostate cancers. Prostate cancer tissue specimens were from a total of 357 patients who were treated for clinically localized prostate cancer by radical prostatectomy or transurethral resection (25). The use of the deidentified archival tissue specimens in research was approved by the Institutional Review Boards of Kaiser Permanente and Thomas Jefferson University. Medical records for the entire cohort had been abstracted once (1999–2001) to ensure uniform criteria for diagnosis, progression, and staging. Hormone therapy was given to 64 of the patients, and the average length of androgen deprivation was 1.56 months (Table 1).

Recurrent human prostate cancers. All specimens were transurethral resections from local recurrences (patients, $n = 198$) and were obtained from Tampere University Hospital in Finland (26). The definition for local recurrence was clinical progression of prostate cancer (development of urethral obstruction after initial favorable response to the therapy). Androgen ablation therapy was given to 127 of the patients, whereas the rest ($n = 71$) had received no hormonal treatment (Table 2).

Immunostaining of prostate cancer cells and paraffin-embedded tissue sections. Immunostaining was performed as described previously (11, 22, 27, 28). The primary antibodies used were the following: phosphorylated (Y^{694}/Y^{699}) Stat5a/b [monoclonal antibody (mAb); Advantex BioReagents; 0.6 μg/mL], total Stat5a/b (mAb; Santa Cruz Biotechnology; 2 μg/mL), and anti-AR (pAb; Santa Cruz Biotechnology; 1:400). Antigen-antibody complexes were detected using appropriate biotinylated goat secondary antibodies (Biogenex Laboratories) followed by streptavidin–horseradish peroxidase complex, using 3,3′-diaminobenzidine as chromogen and Mayer hematoxylin as counterstain.

Table 1. Association between active Stat5a/b and hormone therapy of primary human prostate cancer

	Active Stat5a/b		
	Negative	Positive	*P*
No hormone therapy	124 (42%)	169 (58%)	
Hormone therapy	17 (27%)	47 (73%)	0.02

NOTE: Statistical analysis was performed by two-sided χ^2 test. Hormone therapy: LHRH, $n = 31$; antiandrogen, $n = 2$; LHRH + antiandrogen, $n = 27$; estrogen, $n = 1$; DES, $n = 3$ before surgery (transurethral resection or radical prostatectomy).

Table 2. Active Stat5a/b in recurrent hormone-refractory prostate cancers

	No. patients	%
Recurrent prostate cancers		
Stat5a/b activation status	198	
Negative	52	26
Positive	146	74
Recurrent prostate cancers treated with hormone therapy		
Stat5a/b activation status	127	
Negative	6	5
Positive	121	95

NOTE: Hormone therapy: orchiectomy, $n = 79$; LHRH, $n = 19$; estrogen, $n = 3$; antiandrogen, $n = 1$; orchiectomy + estrogen, $n = 2$; orchiectomy + antiandrogen, $n = 18$; orchiectomy + antiandrogen + estramustine, $n = 1$; LHRH + antiandrogen, $n = 2$; orchiectomy + radiation therapy, $n = 2$.

Scoring of the levels of active Stat5a/b in primary and recurrent clinical human prostate cancers. Individual prostate tumor samples were scored (M.T.N., J.A., and H.L.) for active and nuclear Stat5a/b levels on a scale from 0 to 1, wherein 0 was undetectable and 1 represented positive immunostaining.

Luciferase reporter gene assays. PC-3 cells (0.5×10^5) in Figs. 1A–*D* and 2*A*,*B* and LNCaP prostate cancer cells (0.5×10^6) and T47D breast cancer cells (0.5×10^6) in Figs. 1*E* and 2*C* were transiently cotransfected using FuGENE6 (Roche) with 0.25 μg of each pStat5a or pStat5b, pPrlR, and/or pAR plasmid and either 0.5 μg of pGASx4T109-luciferase, pβ-casein–luciferase, pCIS-luciferase, pCyclin-D1–luciferase, pMMTV-luciferase, or pProbasin-luciferase, and 0.025 μg of pRL-TK (*Renilla* luciferase) as an internal control. The total amount of plasmid DNA per well was normalized by pMod-DNR to 1.275 μg per well. The cells were starved in serum-free medium for 20 h and stimulated with 10 nmol/L human Prl (hPrl) or vehicle in the presence or absence of 0.1, 1, or 10 nmol/L dihydrotestosterone (DHT) in the starvation medium for 16 h. The lysates were assayed for firefly and *Renilla* luciferase activities using the Dual-Luciferase reporter assay system (Promega). Three independent experiments were carried out in triplicate using at least two sets of plasmids that were prepared separately. The firefly luciferase activity was normalized to the *Renilla* luciferase activity of the same sample, and the mean was calculated from the parallels. From the mean values of each independent run, the overall mean and its SE were calculated.

In the experiments of Fig. 2*D*, LNCaP cells (0.5×10^6) were transfected using FuGENE6 (Roche) with a total of 0.525 μg of plasmid DNA (0.5 μg pMMTV-luciferase and 0.025 μg pRL-TK) as described above. After 4 h, the cells were transfected with a total of 200 pmol of control mismatch-antisense or STAT5a/b-antisense oligonucleotides at a final concentration of 100 nmol/L using jetPEI reagent (QBiogene, Inc.). Specifically, Stat5 antisense oligonucleotides (5′-GGG CCT GGT CCA TGT ACG TG-3′, a shared sequence within both human Stat5a and Stat5b transcripts; bp 2153–2173 in open reading frame) were synthesized using a phosphorothioate backbone with 2′-*O*-methoxyethyl modification of five terminal nucleotides (underlined) to increase their stability (ISIS 130826) as described before (ISIS Pharmaceuticals; ref. 29). Mismatch oligonucleotides for the same chemistry were synthesized as a mixture of all four bases. After 24 h, the medium was replaced with serum-free medium for 12 h. The cells were stimulated with 10 nmol/L hPrl and/or 1 nmol/L DHT for 16 h before they were harvested for the luciferase assay described above.

Solubilization of proteins, immunoprecipitation, and immunoblotting. For coimmunoprecipitations of Stat5a/b and AR (Fig. 3*A*), 1.25×10^7 PC-3 cells per immunoprecipitation were cotransfected with 2 μg of pPrlR, pAR, and pStat5a or pStat5b plasmids, serum-starved for 20 h, and then treated with 10 nmol/L hPrl and 1 nmol/L DHT for 16 h. Cells were lysed, and the protein concentrations of clarified tissue lysates were determined as described previously (12, 22). The cell lysates were immunoprecipitated for 3 h at 4°C with anti-Stat5a or anti-Stat5b pAb (both 1.2 μg/mL; Advantex Bioreagents), anti-AR pAb (1.2 μg/mL, C-19; Santa Cruz Biotechnologies), or normal rabbit serum (1.2 μg/mL; Advantex Bioreagents), followed by incubation for 60 min with protein A-Sepharose beads (Pharmacia Biotech). The filters were blotted with anti-Stat5a+b mAb (1:250; Transduction Laboratories, Inc.) or with mAb anti-AR (1:1,000; Biogenex). The immunoreaction was detected by horseradish peroxidase–

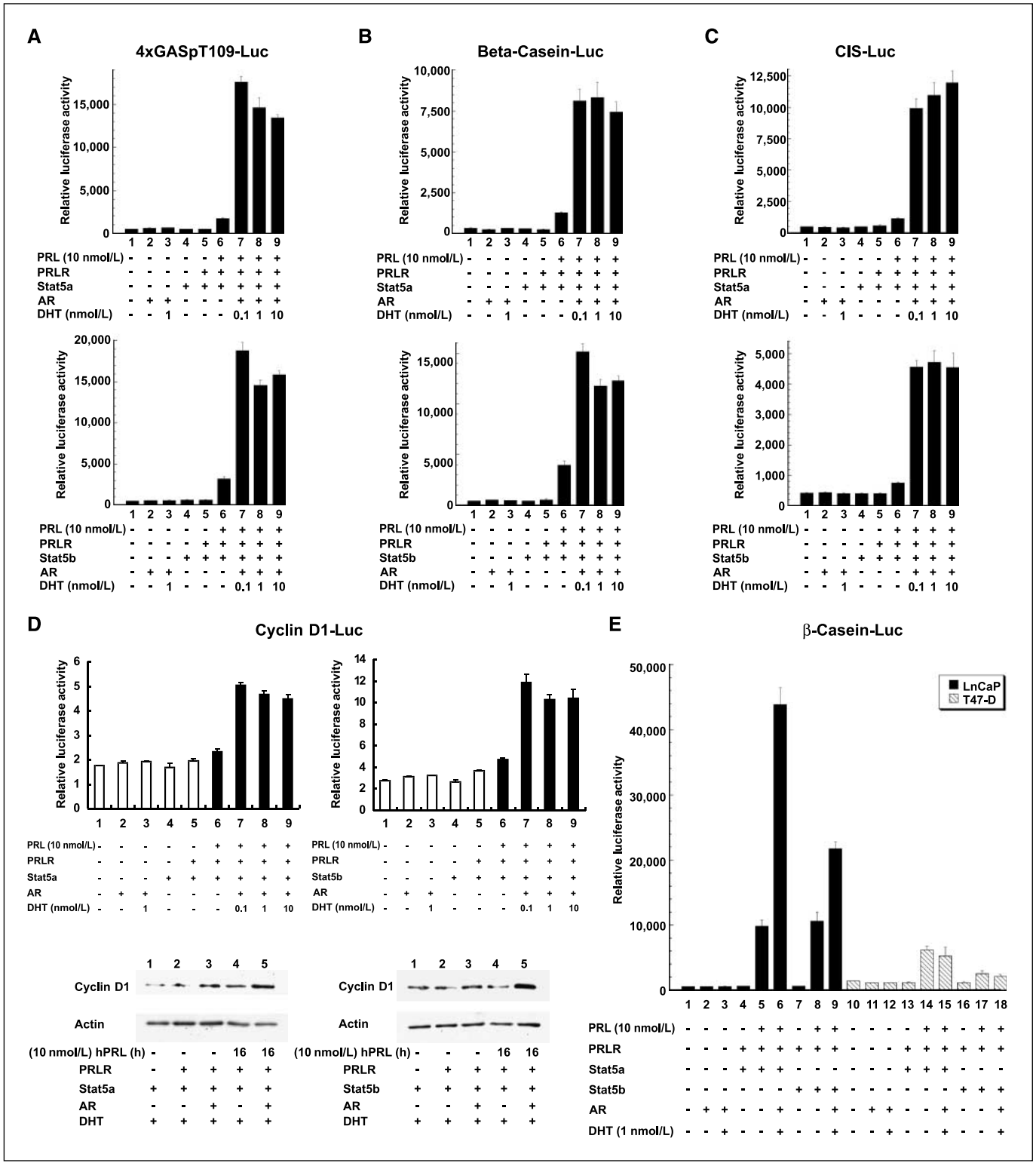

conjugated secondary antibodies in conjunction with enhanced chemiluminescence substrate mixture (Amersham) and exposed to film.

For experiments shown in Fig. 3*C*, LNCaP cells (3×10^7 per immunoprecipitation) were treated with 1 nmol/L DHT in starvation medium for 16 h and then stimulated with hPrl (10 nmol/L) for 15 min. The cell lysates were immunoprecipitated and blotted as described above.

The concentrations of the primary antibodies used in the immunoblottings were the following: anti-AR mAb (1:1,000; Biogenex), anti-Stat5a pAb (Advantex BioReagents; 1:3,000), anti-Stat5b pAb (Advantex BioReagents; 1:3,000), anti-Stat5a+b mAb (1:250; Transduction Laboratories, Inc.), anti-PSA pAb (Dako; 1:1,000), anti-actin pAb (Sigma; 1:4,000), and anti–cyclin D1 (NeoMarkers; 1:200).

Coimmunoprecipitations of FLAG-tagged Stat5a and MYC-tagged AR. Full length Stat5a was amplified by PCR and subcloned to pCMV-3FLAG vector (Stratagene) with an *Eco*R1 and a *Sal*I sites. The full-length AR was amplified by PCR and subcloned to pCMV-3MYC vector (Stratagene) with a *Bam*HI and a *Xho*I sites. Both constructs were subjected to sequencing analysis.

Plasmid pCMV3Flag-Stat5, pCMV3MyC-AR, and pPrlR were cotransfected using FuGENE6 (Roche) into PC-3 cells seeded 24 h earlier (2 μg of each plasmid per 1×10^7 cells; Fig. 3*B*). The cells were starved for 20 h and then stimulated with DHT (1 nmol/L) and hPrl (10 nmol/L) in RPMI 1640 without serum for 16 h. The cell lysates were immunoprecipitated with 25 μL anti-FLAG M2 polyclonal affinity gel (2 μg/mL; Sigma), anti-MYC pAb (1 μg/mL; Upstate), or normal rabbit serum. The primary antibodies were used in the immunoblottings at the following concentrations: anti-FLAG pAb (1:1,000; Stratagene), anti-MYC mAb (1:1,000; Sigma), anti-Stat5a+b mAb (1:250; Transduction Laboratories), and anti-AR mAb (1:1,000; Biogenex) detected by horseradish peroxidase–conjugated secondary antibodies.

Electromobility shift assay. LNCaP cells were transfected with plasmids (0.25 μg of each) expressing AR (pAR), Stat5a (pStat5a), and Prl receptor (PrlR; pPrlR) using FuGENE6 as indicated in Fig. 4*C*. The total amount of plasmid DNA per well was normalized with pMod-DNR. After 18 h, the cells were serum starved for 20 h and then stimulated with 1 nmol/L DHT for 0, 10, or 30 min, or with 1 nmol/L DHT and 10 nmol/L hPrl for 0, 10, or 30 min as indicated. The cell pellets were lysed in 1.5 mL of buffer A (11) and centrifuged (4°C) at $2,300\times g$ for 2 min, and the nuclear pellets were resuspended in 100 μL of high-salt buffer (11) by homogenizing the pellets in a glass homogenizer. After centrifugation at $16,000\times g$, the supernatants were dialyzed in a Slide-a-lyzer mini dialysis unit (Pierce) against 200 mL of dialysis buffer [20 mmol/L HEPES (pH 7.5), 20% glycerol, 100 mmol/L KCl, 0.2 mmol/L EDTA, 5 mmol/L $MgCl_2$, 2 mmol/L DTT, 0.5 mmol/L 2-mercaptoethanol, and 0.5 mmol/L phenylmethylsulfonyl fluoride] for 30 min. Double-stranded AR response element 1 (ARE-1) oligonucleotides (AGCTTGTCTGGTACAGGGTGTTCTTTTGTCGA) were end-labeled with 50 μCi of P^{32} P-ATP (5,000 Ci/mmol) and incubated (1 ng per reaction) with 10 μL of nuclear extracts in the final volume of 20 μL of the binding mixture [50 mmol/L Tris-HCl (pH 7.4), 25 mmol/L $MgCl_2$, 500 mmol/L KCl, 5 mmol/L DTT, 50% glycerol] and 1 μL of 1 mg/mL poly d[(I:C)]. The samples were preincubated with anti-AR antibody (BD BioSciences) or normal rabbit serum as indicated. Polyacrylamide gels (5%) containing 5% glycerol and 0.25× Tris-borate/EDTA were prerun in 0.25× Tris-borate/EDTA buffer at 4 to 10°C for 1.5 h at 300 V. The gels were run at room temperature for 3 h at 250 V, dried, and exposed to X-ray films (X-Omat, Eastman Kodak Co.).

Generation of adenoviruses for gene delivery of wild-type (WT), dominant-negative (DN) Stat5a/b and WT AR. pcDNA-CMV–WT Stat5a/b, pcDNA-CMV–(DN) Stat5a/b, and pAR were cloned to adenoviral vector using BD Adeno-X Expression System 2 (BD Biosciences Clontech) according to the manufacturer's protocol. This specific cloning system was chosen because it uses Cre-loxP–mediated recombination, which reduces the likelihood of development of replication-competent adenovirus over time. The recombinant adenoviruses were purified, linearized by *Pac*I digestion, and transfected to QBI-293A cells to produce infectious recombinant adenoviruses. Viral stocks were expanded in large-scale cultures, purified by double cesium chloride gradient centrifugation, and titered side-by-side by a standard plaque assay method in QBI-293A cells as per the manufacturer's instructions.

Double immunofluorescence cytochemistry of AR and Stat5. PC-3 cells were infected with AdWTStat5a, AdWTPrlR, and AdWTAR each at MOI 4. After 24 h, the cells were plated on collagen-coated culture dishes (MatTek) and serum starved the next day for 12 h before stimulation with 10 nmol/L hPrl for 30 min and/or 1 nmol/L DHT for 60 min. The cells were fixed with 4% PFA and permeabilized with 0.5% Triton X-100, and unspecific staining was blocked with 2% bovine serum albumin in PBS for 1 h. The fixed cells were incubated with anti-Stat5 pAb (Santa Cruz Biotechnology) and anti-AR mAb (Santa Cruz Biotechnology; both at 1:200) followed by goat anti-rabbit fluorescein IgG (Vector Laboratories) and horse anti-mouse Texas Red IgG (Vector Laboratories), respectively (1:150).

Figure 1. AR signaling increases transcriptional activity of Stat5a/b in human prostate cancer cells. *A,* liganded AR increases ligand-induced Stat5a/b reporter gene activity (4XGASpT109-luciferase) in prostate cancer cells. PC-3 cells (0.5×10^5 per well) were transiently cotransfected with a plasmid (0.5 μg) containing a promoter including four Stat5 response elements (GAS) upstream of HSV thymidine kinase promoter (4xGASpT109) coupled to luciferase (*Luc*) plasmid, pRL-TK (*Renilla* luciferase; 0.025 μg), pPrlR (0.25 μg), pStat5a (0.25 μg), pStat5b (0.25 μg), and/or pAR (0.25 μg) as indicated. The total amount of plasmid DNA transfected was normalized to 1.275 μg per well by addition of the empty vector (pMod-DNR). Cells were serum starved for 20 h and then stimulated with DHT in serum-free medium at indicated concentrations and/or hPrl (10 nmol/L) with vehicle controls for 16 h. The cells were harvested, and the relative luciferase activity was determined. *Columns,* mean values of three independent experiments performed in triplicate; *bars,* SE. *B,* transcriptional activity of ligand-induced Stat5a/b in β-casein promoter–luciferase assay is increased in prostate cancer cells by liganded AR. PC-3 cells (0.5×10^5 per well) transiently cotransfected with genomic β-casein promoter–luciferase plasmid (0.5 μg), pRL-TK (0.025 μg), pPrlR (0.25 μg), pStat5a (0.25 μg), pStat5b (0.25 μg), and/or pAR (0.25 μg) as indicated. The total amount of plasmid DNA transfected was normalized to 1.275 μg per well by addition of the empty vector (pMod-DNR). The cells were serum starved for 20 h and treated for 16 h with (+) or without (−) 10 nmol/L hPrl and/or DHT at indicated concentrations. *Columns,* mean values of three independent experiments performed in triplicate; *bars,* SE. *C,* AR signaling increases transcriptional activity of ligand-induced Stat5a/b in prostate cancer cells determined by CIS promoter–luciferase assay. PC-3 cells (0.5×10^5 per well) transiently cotransfected with genomic CIS gene promoter–luciferase reporter gene (0.5 μg), pRL-TK (0.025 μg), pPrlR (0.25 μg), pStat5a (0.25 μg), pStat5b (0.25 μg), and/or pAR (0.25 μg) as indicated. The total amount of plasmid DNA transfected was normalized to 1.275 μg per well by addition of the empty vector (pMod-DNR). The cells were serum starved for 20 h and treated with (+) or without (−) 10 nmol/L hPrl and/or DHT at indicated concentrations for 16 h. *Columns,* mean values of three independent experiments performed in triplicate; *bars,* SE. *D, top,* ligand-induced transcriptional activity of Stat5a/b in cyclin D1 promoter–luciferase assay is increased by AR in prostate cancer cells. PC-3 cells (0.5×10^5 per well) were transiently cotransfected with genomic cyclin D1 gene promoter–luciferase reporter gene (0.5 μg), pRL-TK (0.025 μg), pPrlR (0.25 μg), pStat5a (0.25 μg), pStat5b (0.25 μg), and/or pAR (0.25 μg) as indicated. The total amount of plasmid DNA transfected was normalized to 1.275 μg per well by addition of the empty vector (pMod-DNR). The cells were serum starved for 20 h and treated with (+) or without (−) 10 nmol/L hPrl and/or 0.1, 1, and 10 nmol/L DHT for 16 h. *Columns,* mean values of three independent experiments performed in triplicate; *bars,* SE. *Bottom,* cyclin D1 protein expression is increased in prostate cancer cells that coexpress active AR and active Stat5a/b. LNCaP cells cultured in the presence of DHT (1 nmol/L) were transfected with pPrlR (0.25 μg), pStat5a (0.25 μg), pStat5b (0.25 μg), and/or pAR (0.25 μg) as indicated, serum-starved for 20 h, and treated with vehicle or hPrl (10 nmol/L) for 16 h in the presence of 1 nmol/L DHT in serum-free medium. The total amount of plasmid DNA transfected was normalized to 1.275 μg per well by addition of the empty vector (pMod-DNR). Protein concentrations were calculated, and cyclin D1 protein expression was determined by immunoblotting of the whole cell lysates (35 μg protein per lane) with anti–cyclin D1 mAb. The filters were reblotted with antiactin pAb antibody to show equal loading of the gel. *E,* transcriptional activity of ligand-induced Stat5a/b in β-casein promoter–luciferase assay is increased in LNCaP prostate cancer cells by liganded AR but not in T47D breast cancer cells. LNCaP and T47D cells (0.5×10^6 cells per well) transiently cotransfected with genomic β-casein promoter–luciferase plasmid (0.5 μg), pRL-TK (0.025 μg), pPrlR (0.25 μg), pStat5a (0.25 μg), pStat5b (0.25 μg), and/or pAR (0.25 μg) as indicated. The total amount of plasmid DNA transfected was normalized to 1.275 μg per well by addition of the empty vector (pMod-DNR). The cells were serum starved for 20 h and treated for 16 h with (+) or without (−) 10 nmol/L hPrl and/or 1 nmol/L DHT. *Columns,* mean values of three independent experiments performed in triplicate; *bars,* SE.

The immunofluorescence staining was observed by a Zeiss LSM 510 laser scanning microscope with an Apochromat X63/1.4 oil immersion objective.

Statistics. The probabilities of having active Stat5a/b in primary prostate cancer for patients with or without adjuvant hormone were calculated, and independence between Stat5a/b and hormone therapy was tested using Pearson χ^2 test.

Results

Transcription factor Stat5a/b is active in hormone-refractory recurrent human prostate cancers and during androgen deprivation of primary prostate cancers. Based on our previous results showing that active Stat5a/b in primary human prostate

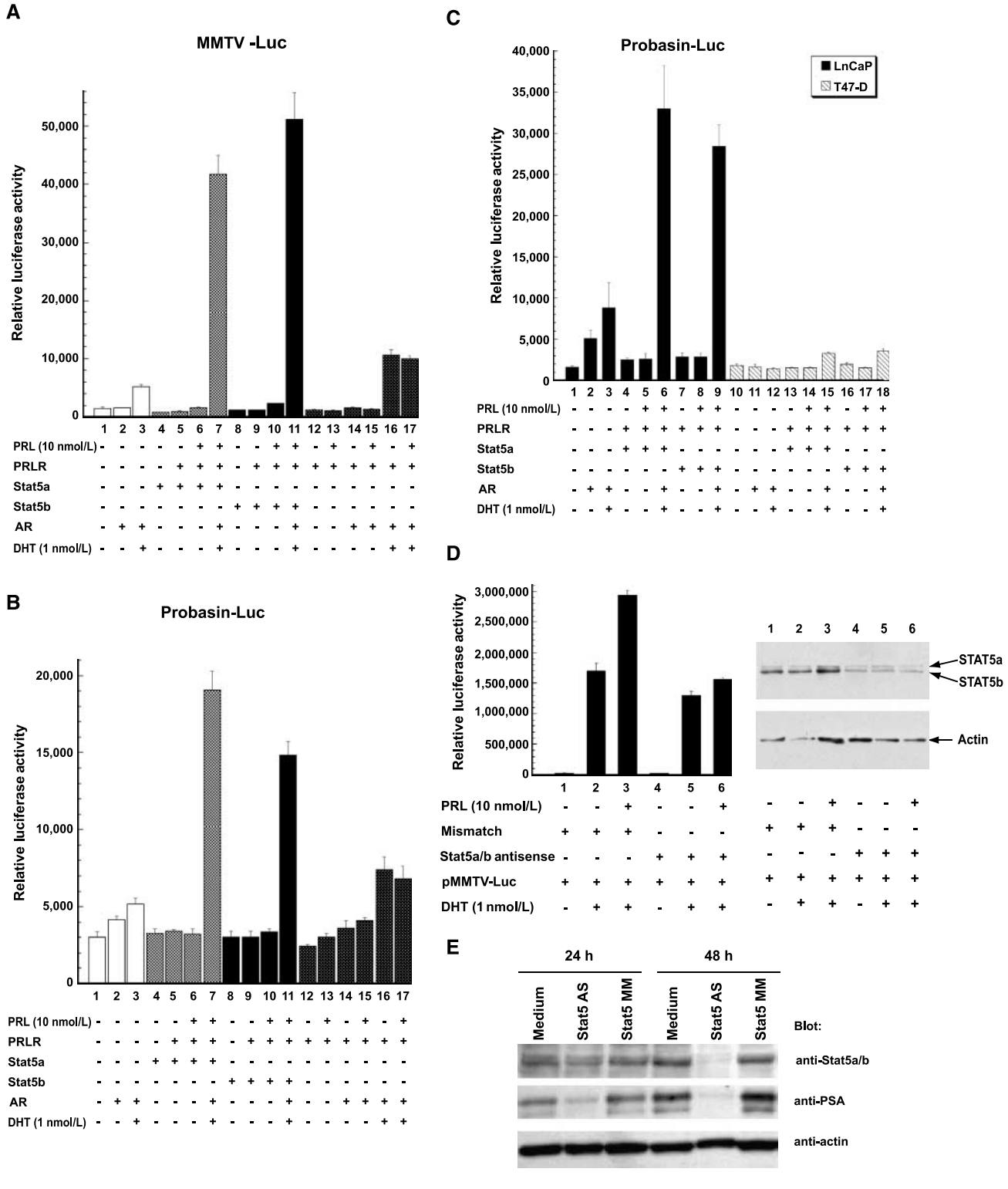

cancer predicted early prostate cancer recurrence (24), we hypothesized that Stat5a/b is constitutively active during androgen deprivation of prostate cancer. To test this hypothesis, we determined Stat5a/b activation during androgen deprivation of both primary and recurrent prostate cancer. First, we assessed the frequency of Stat5a/b activation in primary human prostate cancers from 357 patients. Of these patients, 64 had received androgen deprivation adjuvant therapy for 1.5 months before radical prostatectomy (Table 1). Activation of Stat5a/b was analyzed by immunohistochemical detection of phosphorylated Stat5a/b in paraffin-embedded tissue sections (Supplementary data) as shown previously (11, 12, 22, 24, 27, 28).

In primary prostate cancer, Stat5a/b was more likely to be active if the patient had been treated with androgen ablation before radical prostatectomy ($P = 0.02$) compared with patients who did not receive adjuvant androgen deprivation therapy (Table 1). Specifically, Stat5a/b was almost thrice more likely to be active in prostate cancer of a patient who had been treated with androgen deprivation (Stat5 active, 73% versus Stat5 not active, 27%; $P = 0.02$; Table 1) compared with prostate cancers from patients who did not receive androgen deprivation therapy before radical prostatectomy (Stat5 active, 58% versus Stat5 not active, 42%; $P > 0.05$). There was no significant difference in the distribution of Gleason grades between the two groups. These results show that Stat5a/b is more frequently active in primary prostate cancer during androgen deprivation compared with primary prostate cancers in the presence of circulating androgens.

The observation that Stat5a/b is frequently active in androgen-deprived primary prostate cancers prompted us to ask whether Stat5a/b is also active in hormone-refractory recurrent prostate cancers. To address this question, we first analyzed Stat5a/b activation in tissue specimens obtained by transurethral resection from 198 patients with clinical prostate cancer recurrence (development of urethral obstruction). Significant activation of Stat5a/b was detected in 74% (146 of 198) of all recurrent human prostate cancer specimens (Table 2). Of these patients, 127 had been treated with androgen deprivation before recurrence (see Materials and Methods). Stat5a/b was active in 95% of the 127 recurrent prostate cancer specimens treated with androgen ablation therapy (Table 2). Collectively, these results showed that Stat5a/b is active in the majority of hormone-refractory recurrent prostate cancers.

AR increases transcriptional activity of Stat5 in prostate cancer cells. AR expression persists in prostate cancer cells regardless of prostate cancer progression to hormone refractory stage (30). Our finding showing that Stat5a/b is active in 95% of hormone refractory human prostate cancers led us to test the hypothesis that AR and Stat5a/b signaling pathways interact in prostate cancer cells. First, we tested whether AR affects transcriptional activity of Stat5a/b in prostate cancer cells. Stat5a/b activity was determined using a transiently transfected luciferase reporter gene driven by an artificial promoter containing four Stat5 response elements upstream of HSV thymidine kinase promoter (4xGASpT109; sodium taurocholate cotransporting protein GAS-like elements; ref. 31). Reconstruction of AR and Stat5a/b signaling in PC-3 human prostate cancer cells was chosen as the experimental model for these studies because PC-3 cells do not endogenously express AR or Stat5a/b and because PC-3 cells are of prostate origin, expressing prostate cell–specific coactivators/repressors. Therefore, PC-3 cells provide an unambiguous model for determining the interactions between WT AR and Stat5a/b in prostate cancer cells. In the first set of experiments, PC-3 cells were cotransfected with 4xGASpT109-luciferase, PrlR, Stat5a, or Stat5b, and/or AR, serum-starved for 20 h, and stimulated with hPrl (10 nmol/L) and/or DHT at concentrations of 0.1, 1, and 10 nmol/L for 16 h. Upon coexpression of active Stat5a/b with DHT-stimulated AR, Prl-induced transcriptional activity of Stat5a was increased by 7-fold to 9-fold and of Stat5b by 5-fold to 6-fold in prostate cancer cells (Fig. 1*A, lanes 7–9*) compared with cells negative for AR (Fig. 1*A, lane 6*).

Because activity of transcription factors and nuclear receptors is dependent on a specific promoter context, we extended the determination of Stat5a/b activity from the artificial promoter to genomic promoters regulated by Stat5a/b. We chose for the next set of experiments β-casein–luciferase, cyclin D1–luciferase, and CIS (cytokine inducible SH2-containing protein)–luciferase reporter genes. β-casein and cyclin D1 promoters both contain a Stat5-binding site flanked by a nonconsensus Stat5a/b site, and therefore, they constitute strong tetrameric Stat5-binding promoters (32, 33). The promoter of CIS contains four consensus Stat5a/b recognition sequences. In PC-3 cells coexpressing

Figure 2. Stat5a/b signaling increases transcriptional activity of AR in human prostate cancer cells. *A,* transcriptional activity of AR in MMTV promoter–luciferase assay is increased in prostate cancer cells expressing active Stat5a/b. PC-3 cells (0.5×10^5 per well) were transfected with MMTV-luciferase plasmid (0.5 μg), pRL-TK (0.025 μg), pPrlR (0.25 μg), pAR (0.25 μg), pStat5a (0.25 μg), and/or pStat5b (0.25 μg) as indicated. Cells were serum starved for 20 h and then treated with (+) or without (−) 10 nmol/L hPrl and/or 1 nmol/L DHT in serum-free medium for 16 h. *Columns,* mean values of three independent experiments; *bars,* SE. *B,* active Stat5a/b signaling pathway increases transcriptional activity of AR determined by probasin-luciferase assay in human prostate cancer cells. PC-3 cells were transfected with genomic probasin promoter–luciferase reporter gene (0.5 μg), pRL-TK (0.025 μg), pPrlR (0.25 μg), pAR (0.25 μg), pStat5a (0.25 μg), or pStat5b (0.25 μg) as indicated. Cells were serum starved for 20 h and then treated with (+) or without (−) 10 nmol/L hPrl and/or 1 nmol/L DHT in serum-free medium for 16 h. *Columns,* mean values of three independent experiments; *bars,* SE. *C,* transcriptional activity of liganded AR in probasin promoter–luciferase assay is increased in LNCaP prostate cancer cells by ligand-induced Stat5a/b but not in T47D breast cancer cells. LNCaP prostate cancer cells and T47D breast cancer cells (0.5×10^6 per well) were transfected with genomic probasin promoter–luciferase reporter gene (0.5 μg), pRL-TK (0.025 μg), pPrlR (0.25 μg), pAR (0.25 μg), pStat5a (0.25 μg), or pStat5b (0.25 μg) as indicated. Cells were serum-starved for 20 h and then treated with (+) or without (−) 10 nmol/L hPrl and/or 1 nmol/L DHT in serum-free medium for 16 h. *Columns,* mean values of three independent experiments; *bars,* SE. *D,* endogenously expressed active Stat5 increases transcriptional activity of liganded AR in LNCaP cells. *Left,* LNCaP cells (0.5×10^6 per well) were transfected with a total of 0.525 μg of plasmid DNA (0.5 μg pMMTV-Luc and 0.025 μg pRL-TK). Four hours after DNA transfection, the cells were transfected with a total of 200 pmol of control mismatch or STAT5a/b antisense oligonucleotides at a final concentration of 100 nmol/L. After 24 h, the medium was replaced with starvation medium for 12 h. The cells were then treated with 10 nmol/L hPrl and/or 1 nmol/L DHT for 16 h and harvested for the luciferase assay. Antisense inhibition of Stat5 blocks the transcriptional synergy between endogenously expressed Stat5 and AR in LNCaP cells treated with hPrl and DHT. *Right,* cells in parallel wells were harvested and lysed 24 h after transfection with Stat5a/b antisense or mismatch oligonucleotides. The total amount of protein was determined by modified Bradford assay, and the total amount of Stat5a/b protein was detected by blotting the membrane with anti-Stat5a+b mAb (1:250). The lower part of the filter was blotted with antiactin pAb to show equal loading of the gels. *E,* PSA protein expression is decreased in LNCaP prostate cancer cells if Stat5a/b expression is inhibited. Stat5a/b expression was inhibited in LNCaP cells (1×10^6 per well) cultured in the presence of DHT (1 nmol/L) by transfection of the cells with Stat5a/b antisense oligonucleotides (900 pmol per well) for 24 or 48 h with mismatch oligonucleotides or culture medium as controls. Whole-cell lysates (35 μg protein per lane) were immunoblotted with anti-PSA antibody. The upper part of the filter was blotted with anti-Stat5a/b antibody (1:250) to show effective Stat5a/b protein inhibition and the lower parts of the filters were blotted with anti-PSA pAb (1:1,000) and antiactin pAb (1:4,000).

liganded AR with active Stat5a or Stat5b and PrlR, ligand-induced transcriptional activity of Stat5a/b in β-casein–luciferase assay was increased by 3-fold to 6-fold and in CIS-luciferase assay by 7-fold to 10-fold (Fig. 1*B* and *C, lanes 7–9*) compared with cells negative for AR (Fig. 1*B* and *C, lane 6*). When assayed with cyclin D1–luciferase, Prl-induced transcriptional activity of Stat5a/b was increased by 2-fold to 3-fold in cells expressing liganded AR in addition to Stat5a or Stat5b compared with cells negative for active AR (Fig. 1*D*, compare *lanes 7–9* to *lane 6*). To extend the findings to the protein level, we used cyclin D1 protein expression as a quantifiable indicator of Stat5 transcriptional activity in LNCaP cells transfected with PrlR, Stat5a/b, and/or AR (Fig. 1*D, bottom*). In line with the results obtained from the Stat5-regulated gene assays, levels of cyclin D1 protein were increased if prostate cancer cells expressed both active Stat5a or Stat5b and liganded AR (Fig. 1*D, bottom, lane 5*) compared with DHT-stimulated AR only (*lane 3*) or cells expressing Prl-activated Stat5a/b only (*lane 4*). In addition to PC-3 cells, synergy between active Stat5a/b and AR in induction of Stat5a/b driven transcription in β-casein promoter reporter gene assay was also evident in LNCaP cells cotransfected with AR, PrlR, and Stat5a or Stat5b (Fig. 1*E*, compare *lane 6* to *lane 5* and *lane 9* to *lane 8*). In contrast, no coaction between Stat5a/b and AR was observed in T47D human breast cancer cells transfected with the same plasmids. This result suggested that prostate cell–specific factors may be required for the transcriptional synergy between AR and Stat5a/b. Taken together, the data presented here indicate for the first time that liganded AR, even at low levels of androgens, increases transcriptional activity of Stat5a/b in prostate cancer cells.

Stat5a/b signaling increases transcriptional activity of liganded AR in prostate cancer cells. Our observations of transcriptional activity of Stat5a/b being regulated by AR suggested an interaction between AR and Stat5a/b in prostate cancer cells. This made us focus our investigation next on determining whether active Stat5a/b signaling affects transcriptional activity of AR in prostate cancer. We tested this in PC-3 cells using a transiently transfected luciferase reporter gene driven by androgen-regulated promoters mouse mammary tumor virus (MMTV; ref. 34) or a genomic probasin promoter (35). PC-3 cells cotransfected with MMTV-luciferase, PrlR, Stat5a or Stat5b, and/or AR were serum starved for 20 h and stimulated with hPrl (10 nmol/L) and/or DHT (1 nmol/L) in serum-free medium for 16 h. Compared with Stat5a/b-negative cells, coexpression of active Stat5a or Stat5b with PrlR and AR in prostate cancer cells led to an 8-fold increase in DHT-induced transcriptional activity of AR (Fig. 2*A*, compare *lanes 7* and *11* to *lane 3*) using MMTV-luciferase as a quantifiable indicator of AR transcriptional activity. Similarly, probasin-luciferase assay showed a 4-fold increase in ligand-induced transcriptional activity of AR in the cells coexpressing active Stat5a or Stat5b in addition to PrlR and AR versus AR only–expressing cells (Fig. 2*B*, compare *lanes 7* and *11* to *lane 3*). Synergy between transfected Stat5a/b and AR was observed in LNCaP prostate cancer cells as well, but not in T47D human breast cancer cells cotransfected with probasin-luciferase, PrlR, AR, and Stat5a or Stat5b (Fig. 2*C*) suggesting prostate cell specificity for the cooperative interaction between Stat5a/b and AR on AR-regulated gene transcription.

Next, we tested synergy between endogenously expressed Stat5 and AR in human prostate cancer cells (Fig. 2*D*). LNCaP cells, transfected with MMTV-luciferase, served as a model system in these experiments because LNCaP cells express both Stat5a/b and AR. After 24 h, the cells were serum starved for 12 h and stimulated with hPrl (10 nmol/L) and/or DHT (1 nmol/L) for 16 h before the MMTV-luciferase assay. Treatment of the cells with both DHT and Prl increased transcriptional activity of AR by 80% (Fig. 2*D, left*, compare *lane 3* to *lane 2*), suggesting a positive coaction between endogenously expressed Stat5a/b and AR in prostate cancer cells. To verify that Stat5a/b is critical for the enhancement of AR transcriptional activity by Prl in LNCaP cells, we inhibited Stat5a/b expression by Stat5a/b antisense oligonucleotides, which was shown by Western blotting of the whole cell lysates (Fig. 2*D, top right*). Mismatch oligonucleotides were used as control, and the filters were reblotted with antiactin pAb to show equal loading of the gels. Importantly, inhibition of Stat5a/b expression by Stat5a/b antisense oligonucleotides blocked the increase of Prl-induced transcriptional activity of AR (Fig. 2*D, left, lanes 5* and *6*).

To validate the significance of Stat5a/b signaling on transcriptional activity of AR at the protein expression level, we tested whether Stat5a/b contributes to PSA protein expression in prostate cancer cells. LNCaP cells were chosen as the experimental model because they are positive for Stat5a/b and AR and express PSA under the regulation of androgens. LNCaP cells cultured in the presence of DHT (1 nmol/L) were transiently transfected with Stat5a/b antisense oligonucleotides for 24 and 48 h. The level of PSA protein expression in LNCaP cells was decreased by ~90% if Stat5a/b expression was inhibited by Stat5a/b antisense oligonucleotides at 48 h versus control (mismatch oligonucleotides; Fig. 2*E*). These results suggest that functional synergy between Stat5a/b and AR is reflected on AR-driven protein expression in LNCaP prostate cancer cells.

AR and Stat5a/b physically interact in prostate cancer cells. To identify the molecular mechanisms underlying the mutually stimulatory interaction between Stat5a/b and AR in prostate cancer cells, we first examined whether Stat5a/b and AR physically interact in human prostate cancer cells. PC-3 cells were cotransfected with PrlR, AR, and Stat5a or Stat5b, serum starved for 20 h, and then stimulated with hPrl (10 nmol/L) and DHT (1 nmol/L) for 16 h. AR was immunoprecipitated from the cell lysates and blotted with a mAb recognizing both Stat5a and Stat5b. Stat5a (94 kDa) and Stat5b (92 kDa) formed a complex with AR in prostate cancer cells (Fig. 3*A, i, lanes 1* and *2*). Control immunoprecipitations with normal rabbit serum gave a band at 94 kDa, which was significantly weaker than the 94-kDa band yielded with Stat5a-specific antibody. In the converse experiments, immunoprecipitated Stat5a and Stat5b were blotted with a mAb recognizing AR yielding a band at 110 kDa. This suggested that liganded AR formed a complex with active Stat5a and Stat5b in prostate cancer cells (Fig. 3*A, ii, lanes 5* and *6*). The weaker band under the 110-kDa AR in lane 5 (Fig. 3*A, ii*) likely resulted from *in vitro* proteolytic cleavage of AR, which has been described in prostate cancer cells previously (36).

In a parallel set of experiments, we cloned Stat5a and AR into FLAG-tagged and MYC-tagged expression vectors, respectively. PC-3 cells were transfected with pAR-MYC and pStat5a-FLAG in addition to pPrlR as described in the Materials and Methods. After serum starvation for 20 h, the cells were treated with DHT (1 nmol/L) and hPrl (10 nmol/L) for 16 h. Complex formation between Stat5 and AR was shown by immunoprecipitation of 3FLAG-STAT5a with anti-FLAG M2 antibody coupled gel and by blotting with mAb recognizing c-MYC tag (Fig. 3*B, i, lane 1*). The immunoprecipitation with normal rabbit serum was loaded in

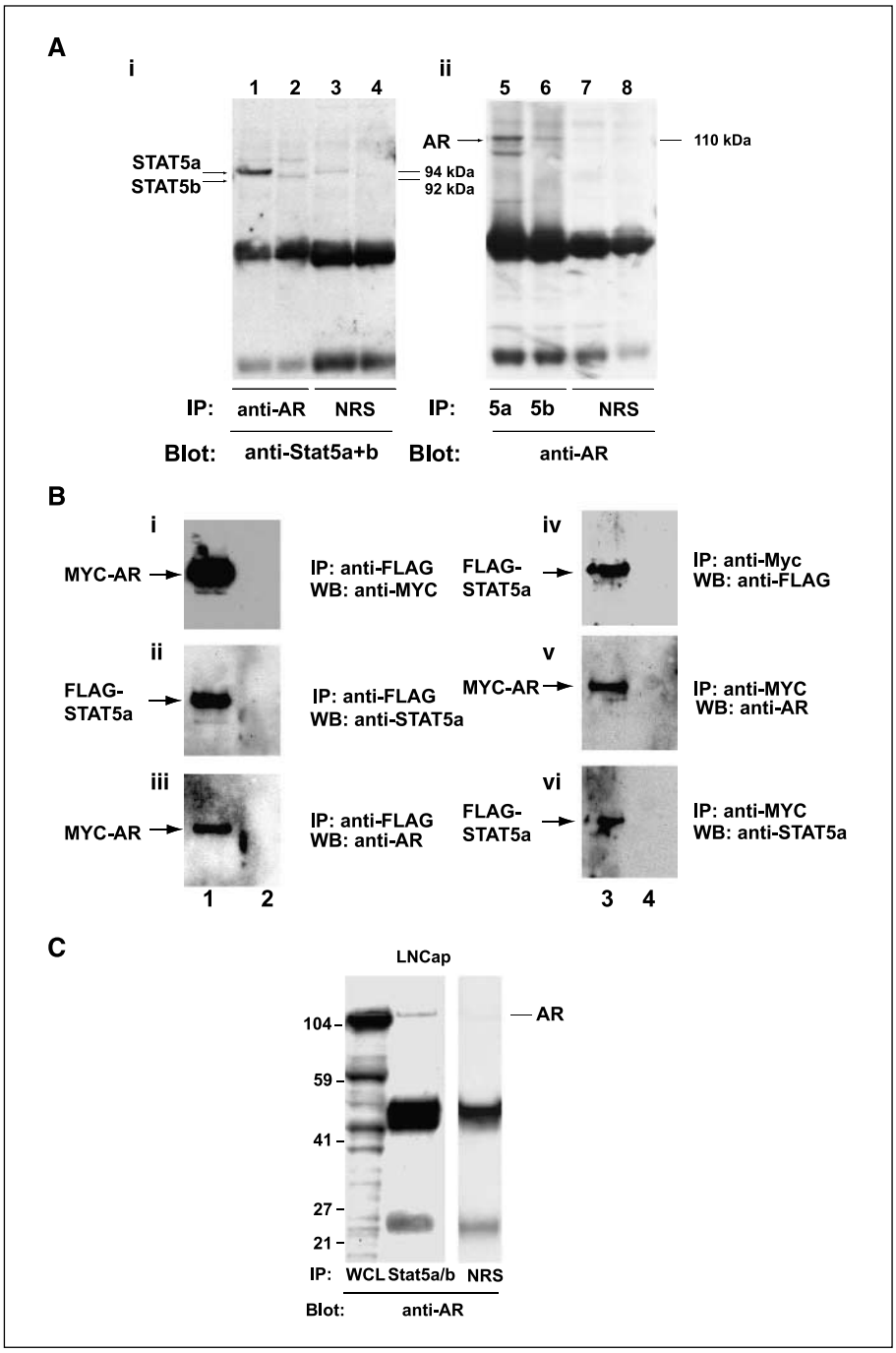

Figure 3. Stat5a/b and AR physically interact in prostate cancer cells and reciprocally promote localization of one another. *A,* Stat5a/b and AR form a complex in prostate cancer cells as shown by immunoprecipitation and immunoblotting. PC-3 cells were cotransfected with pPrlR, pStat5a, and pAR (*lanes 1, 3, 5,* and *7*) or pPrlR, pStat5b, and pAR (*lanes 2, 4, 6,* and *8*; 2 μg of each plasmid per 1.25×10^7 cells), serum-starved for 20 h, then stimulated with 10 nmol/L hPrl and 1 nmol/L DHT for 16 h. AR was immunoprecipitated with a pAb against AR (*lanes 1* and *2*) with normal rabbit serum as control (*lanes 3* and *4*) and blotted with an anti-Stat5a+b mAb (*lanes 1–4*). Stat5a (94 kDa) and Stat5b (92 kDa) formed a complex with AR in prostate cancer cells (*lanes 1* and *2*, respectively). In the converse experiments, Stat5a and Stat5b were immunoprecipitated with pAb against Stat5a or Stat5b (*lanes 5* and *6*, respectively) with normal rabbit serum as control (*lanes 7* and *8*). Immunoprecipitations were blotted with a monoclonal antibody recognizing AR (110 kDa; *lanes 5–8*). *B,* pCMV-3FLAG-STAT5a, pCMV-3MYC-AR, and pPrlR plasmids (2 μg of each plasmid per 1.0×10^7 cells) were cotransfected to PC-3 cells. The cells were starved for 20 h and stimulated with 1 nmol/L DHT and 10 nmol/L hPrl in RPMI 1640 without serum for the next 16 h. 3FLAG-STAT5a was immunoprecipitated with a polyclonal anti-FLAG M2 affinity gel (0.0025 μg; *i–iii, lane 1*) and with normal rabbit serum (7.5 μL) as control (*i–iii, lane 2*) and blotted with an anti-MYC mAb (1:1,000; *i, lanes 1* and *2*). 3MYC-AR formed a complex with 3FLAG-STAT5a in prostate cancer cells (*i, lane 1*). The coimmunoprecipitation of FLAG-STAT5a and 3MYC-AR was confirmed by stripping and reblotting the membrane with an anti-STAT5a+b mAb (1:250; *ii*) and an anti-AR mAb (1:1,000; *iii*), respectively. 3MYC-AR was immunoprecipitated with 7.5 μL of an anti-MYC pAb (*iv–vi, lane 3*), with normal rabbit serum as control (*iv–vi, lane 4*) and blotted with an anti-FLAG mAb (1:1,000; *iv, lanes 3* and *4*). The immunoprecipitation of 3MYC-AR and coimmunoprecipitation of 3FLAG-STAT5a was confirmed by stripping and reblotting the membrane with an anti-AR mAb (1:1,000; *v*) and an anti-STAT5a+b mAb (1:250; *vi*), respectively. *C,* physical interaction of endogenously expressed Stat5a/b and AR in LNCaP human prostate cancer cells. LNCaP cells (3×10^7 per immunoprecipitation) were treated with 1 nmol/L DHT for 16 h in starvation medium. The cells were stimulated with 10 nmol/L hPrl for 15 min, and Stat5a/b was immunoprecipitated with an anti-Stat5a/b pAb (1.2 μg/mL) or normal rabbit serum (1.2 μg/mL). The membranes were blotted with an anti-AR mAb (1:1,000). Whole-cell lysate (*WCL*) of LNCaP cells shows the endogenous AR expression in LNCaP cells.

lane 2. The immunoprecipitation of 3FLAG-STAT5a and coimmunoprecipitation of 3MYC-AR were validated by stripping and reblotting the membrane with anti-STAT5a mAb (Fig. 3*B, ii, lane 1*) and anti-AR mAb (Fig. 3*B, iii, lane 1*), respectively. Conversely, immunoprecipitation of the cell lysates with anti-MYC pAb yielded a 118-kDa protein corresponding to the FLAG-tagged STAT5a, as shown by immunoblotting with anti-FLAG mAb (Fig. 3*B, iv, lane 3*). The immunoprecipitation with normal rabbit serum was loaded in lane 4. The immunoprecipitation of 3Myc-AR and coimmunoprecipitation of 3FLAG-STAT5a was validated by stripping and reblotting the membrane with anti-AR mAb (Fig. 3*B, v, lane 3*) and anti-STAT5a (Fig. 3*B, vi, lane 3*) mAb, respectively.

In the third set of experiments (Fig. 3*C*), we investigated whether endogenously expressed Stat5a/b and AR in human prostate cancer cells physically interact when activated. LNCaP cells were treated with DHT (1 nmol/L) in starvation medium for 16 h and with hPrl (10 nmol/L) for 15 min before harvesting the cells. Stat5a/b was immunoprecipitated using anti-Stat5a/b pAb with normal rabbit serum as control and blotted with a monoclonal antibody against AR. Immunoprecipitation of Stat5a/b pulled down a 110-kDa protein recognized by anti-AR antibody (Fig. 3*C*), which was absent in the cell lysates immunoprecipitated with normal rabbit serum indicating physical interaction between endogenously expressed Stat5a/b and AR in LNCaP cells upon ligand stimulation. The results of these studies indicate that activated Stat5a/b and liganded AR physically interact in prostate cancer cells.

AR increases nuclear localization of Stat5a/b in human prostate cancer cells. Neither Stat5a/b or AR possess kinase activity and therefore are not likely to promote transcriptional activity of each other through increased protein phosphorylation. To search for alternative molecular mechanisms underlying synergy of AR and Stat5a/b in prostate cancer cells, we hypothesized that nuclear translocation of active Stat5a/b is altered by the presence of liganded AR in prostate cancer cells. To test this, PC-3 cells were cotransfected with PrlR and Stat5a with or without cotransfection of AR, serum-starved for 20 h, treated with DHT (1 nmol/L) for 16 h, and stimulated with hPrl (10 nmol/L) for 0, 10, or 60 min. In the absence of added hPrl, Stat5a was predominantly found in the cytoplasm of PC-3 cells transfected with PrlR and Stat5a (Fig. 4*A, i*). As expected, addition of hPrl (10 nmol/L) led to nuclear translocation of Stat5a at 10 min with maximal immunostaining of Stat5a in the nucleus at 60 min (Fig. 4*A, ii* and *iii*). However, if the cells coexpressed liganded AR in addition to Stat5a and PrlR, stimulation of the cells with Prl resulted in remarkably more intense nuclear immunostaining for Stat5a at 10 and 60 min (Fig. 4*A, v* and *vi*) compared with the cells stimulated with Prl but expressing only Stat5a and PrlR (Fig. 4*A, ii* and *iii*). Unexpectedly, there was also evidence of active Stat5 in the nuclei in the absence of hPrl stimulation if the cells coexpressed liganded AR (Fig. 4*A, iv*). These results suggest that nuclear translocation of Stat5a/b is enhanced by liganded AR.

To further investigate the effect of AR on nuclear translocation of Stat5a/b, we setup double immunostaining of Stat5a/b and AR by indirect immunofluorescence in prostate cancer cells. Stat5a, AR, and PrlR were expressed in PC-3 cells using replication-deficient adenovirus as an expression vector, as previously shown (12, 22). After serum starvation for 12 h, the cells were stimulated with hPrl (10 nmol/L) for 30 min and/or DHT (1 nmol/L) for 60 min. As shown in Fig. 4*B*(*i–iv*), when PC-3 cells were not stimulated with hPrl or DHT, Stat5a (*green*) was located in the cytoplasm of the cells (Fig. 4*B, i*). As expected, when PC-3 cells were stimulated with hPrl for 30 min, Stat5 was translocated to the nuclei of the cells (Fig. 4*B, ii*). Importantly, if the cells were simultaneously stimulated with both hPrl and DHT, the nuclear immunostaining of Stat5a was the most intense (Fig. 4*B, iv*). Intriguingly, stimulation of the cells with DHT induced nuclear translocation of Stat5a in the absence of hPrl stimulation of the cells (Fig. 4*B, iii*). In summary, the results of these experiments shown in Fig. 4*B*(*i–iv*) support the novel concept that liganded AR enhances nuclear translocation of Stat5a/b in prostate cancer cells.

Active Stat5a/b increases nuclear localization of AR in human prostate cancer cells. In the next set of experiments, we asked whether accumulation of DHT-induced AR in the nuclear compartment is affected by active Stat5a/b in prostate cancer cells (Fig. 4*C*). PC-3 cells were cotransfected with AR with or without transfection of PrlR and Stat5a, serum-starved for 20 h, treated with hPrl (10 nmol/L) for 16 h, and then stimulated with DHT (1 nmol/L) for 0, 10, or 60 min. In the absence of the ligand (DHT), AR was predominantly located in the cytoplasm of PC-3 cells transfected with AR only (Fig. 4*C, i*). Weak nuclear AR immunostaining was detected at 10 min with maximal nuclear immunostaining detected at 60 min after stimulation with DHT as expected (Fig. 4*C, ii–iii*). In cells expressing activated Stat5a and PrlR in addition to AR, strong punctate nuclear immunostaining of AR was already evident at 10 min after DHT stimulation of PC-3 cells (Fig. 4*C, v*). At 60 min after DHT stimulation, immunostaining of AR in subnuclear foci (37) was significantly more intense in cells expressing active Stat5a and AR compared with cells expressing AR only (Fig. 4*C, vi*). A weak nuclear immunostaining of unliganded AR was visible in cells expressing ligand-induced active Stat5 (Fig. 4*C, iv*).

We next analyzed the AR immunofluorescence staining for AR as described in Fig. 4*B*. In the absence of DHT stimulation, AR (*red*) was located in the cytoplasm of the cells (Fig. 4*B, v*). When PC-3 cells were stimulated with DHT, AR was translocated to the nuclei of PC-3 cells as expected (Fig. 4*B, vii*). Importantly, the nuclear immunostaining of Stat5 and AR was the most intense if the cells were simultaneously stimulated with both hPrl and DHT (Fig. 4*B, viii*). Stimulation of the cells with hPrl induced nuclear translocation of not only Stat5 (Fig. 4*A, ii*) but also AR (Fig. 4*B, vi*). In conclusion, the results of these experiments (Fig. 4*B* and *C*) provide evidence that activated Stat5a/b enhances nuclear translocation of AR in prostate cancer cells.

Finally, to examine whether DNA binding of AR is affected by active Stat5a/b, we performed EMSA analysis of AR in LNCaP cells. LNCaP cells were transfected with AR alone or with plasmids encoding AR, PrlR, and Stat5a, and the total amount of plasmid DNA was normalized by addition of the empty vector. After transfection (18 h), the cells were serum-starved for 20 h, stimulated with DHT (1 nmol/L) and hPrl (10 nmol/L) for 0, 10, and 30 min, and the nuclear extracts were isolated (Fig. 4*D*). The ARE-1 was used as a probe, and the ability of anti-AR antibody to supershift DNA-bound AR in LNCaP cells was verified (Fig. 4*D, lanes 7* and *8*). Stimulation of LNCaP cells with DHT induced binding of AR to DNA at 10 and 30 min as expected (Fig. 4*D, lanes 2* and *3*). When LNCaP cells were transfected with not only AR but also with Stat5a and PrlR and stimulated with both DHT and hPrl for 30 min, the binding of AR to DNA was increased by 2-fold to 3-fold as determined by EMSA (Fig. 4*D*, compare *lanes 2* and *3* to *lanes 5* and *6*). This result further supports the concept that active

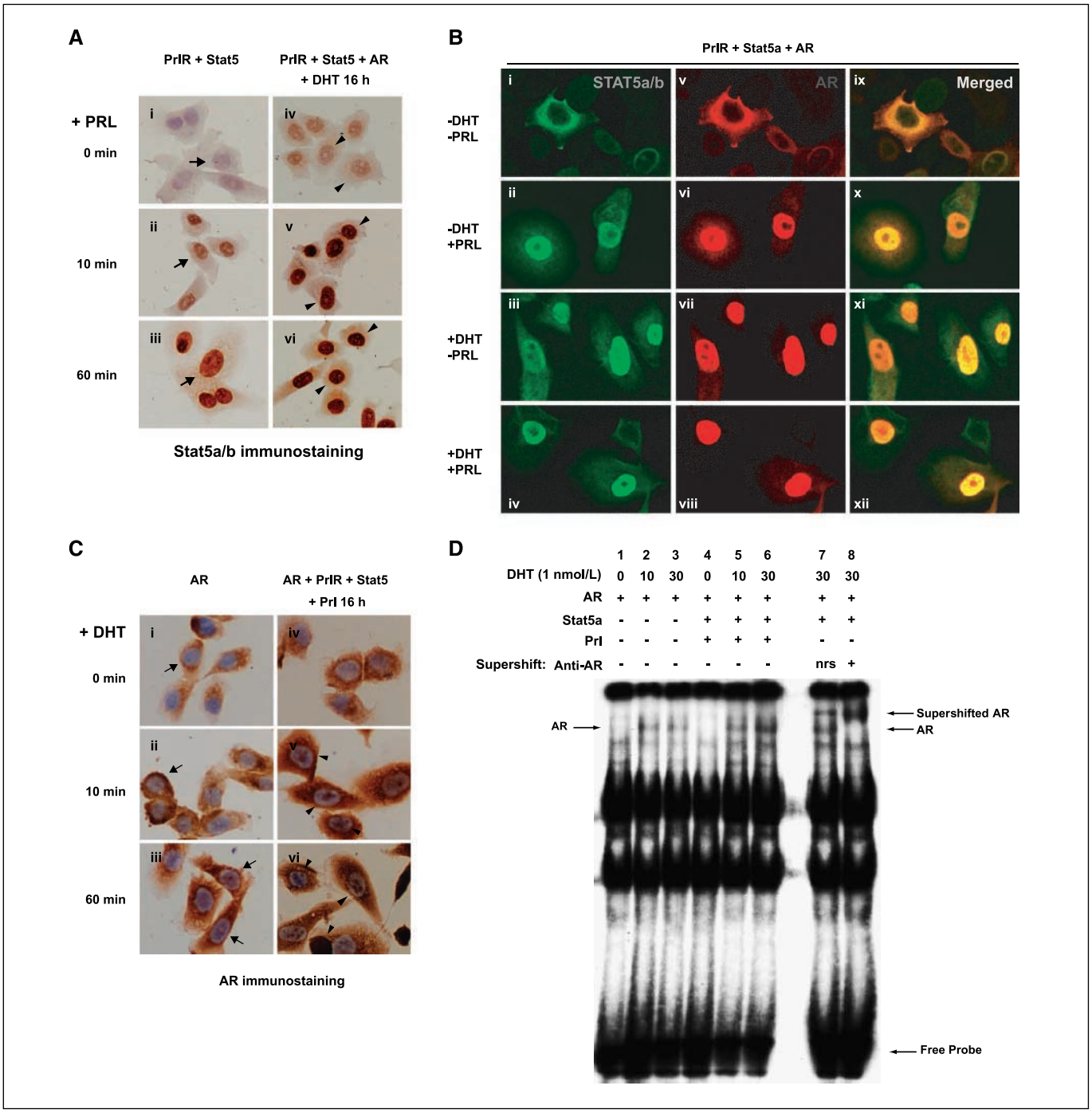

Figure 4. Liganded AR and active Stat5a/b increase nuclear localization of each other in prostate cancer cells. *A,* liganded AR increases ligand-induced nuclear translocation of Stat5a in prostate cancer cells. PC-3 cells were cotransfected with 0.25 μg of pPrlR and pStat5a without (*i–iii*) or with pAR (0.25 μg; *iv–vi*). The total amount of transfected plasmid was normalized by addition of the empty vector (pMod-DNR). The cells were serum starved for 20 h, treated with 1 nmol/L DHT for 16 h, stimulated with 10 nmol/L hPrl for 0, 10, or 60 min, fixed, and immunostained for Stat5a/b. Immunostaining for Prl-induced Stat5a/b in the nuclear compartment of the cells was more intense if the cells expressed both liganded AR and active Stat5a (*arrowheads*) compared with cells expressing only active Stat5a (*arrows*). *B,* double immunostaining of Stat5a and AR by indirect immunofluoresence in prostate cancer cells. PC-3 cells were infected with replication-deficient adenovirus expressing WT Stat5a (AdWTStat5a; MOI = 4), WT hPrlR (AdhPrlR; MOI = 4), and WT AR (AdWTAR; MOI = 4), serum-starved (0% FCS) for 12 h before stimulation of the cells with 10 nmol/L hPrl for 30 min and/or 1 nmol/L DHT for 60 min. After stimulation with hPrl and DHT, the cells were immunostained for Stat5 (*green*; *i–iv*) and AR (*red*; *v–viii*). *C,* active Stat5 signaling pathway increases ligand-induced nuclear translocation of AR in prostate cancer cells. PC-3 cells were cotransfected with pAR (0.25 μg) without (*i–iii*) or with 0.25 μg of pPrlR and pStat5a (0.25 μg; *iv–vi*), serum starved for 20 h, treated with 10 nmol/L hPrl for 16 h, and stimulated with 1 nmol/L DHT for 0, 10, or 60 min. The prostate cancer cells were fixed and immunostained for AR. Note a more intense, punctate immunostaining for AR in the cells expressing both active Stat5a and AR (*arrowheads*) compared with cells that express AR only (*arrows*). *D,* binding of DHT-induced AR to DNA is increased in LNCaP human prostate cancer cells that express active Stat5a shown by EMSA analysis. LNCaP cells were transfected with pAR (0.25 μg) or with pAR (0.25 μg), pStat5a (0.25 μg), and pPrlR (0.25 μg). The total amount of plasmid DNA per well was normalized with pMod-DNR. After 18 h, the cells were serum starved for 20 h and then stimulated with 1 nmol/L DHT for 0, 10, or 30 min in the presence or absence of 10 nmol/L hPrl in the serum-free culture medium. The cells were harvested, and the nuclear extracts were isolated and incubated with normal rabbit serum or with an antibody against AR before incubation with the oligonucleotide probe corresponding to ARE-1. *Arrow,* the complex that binds to ARE-1. The complex was supershifted by antibody against AR (*lane 8*).

Stat5 enhances transcriptional activity of AR and that active Stat5 and AR increase nuclear localization of each other in human prostate cancer cells.

Discussion

The median duration of response to hormonal ablation therapy of primary prostate cancer in patients is <3 years (30). Although the use of androgen blockade in the treatment of prostate cancer has expanded in the last decade, the molecular mechanisms underlying the development of androgen-independent disease are still largely unclear and no effective therapy for hormone-refractory prostate cancer presently exists. Importantly, we establish here cooperative interaction between AR and Stat5a/b in prostate cancer cells. We propose that Stat5a/b and AR are two survival signaling pathways that transcriptionally synergize with one another in human prostate cancer.

We have shown previously that Stat5a/b is critical for the viability of human prostate cancer cells (22) and that Stat5a/b is activated in prostate cancer but not in normal human prostate epithelium (22). Furthermore, activation of Stat5a/b in primary prostate cancer predicted early prostate cancer recurrence (12, 24). The key result of the work presented here is the cooperative interaction between Stat5a/b and AR signaling in prostate cancer. Specifically, we showed that active Stat5a/b increased transcriptional activity of AR in prostate cancer cells. We further showed that liganded AR, in turn, increased transcriptional activity of Stat5a/b in human prostate cancer cells. Our findings of synergic interaction between Stat5a/b and AR were consistent in a battery of natural Stat5-responsive and AR-responsive promoters, suggesting that Stat5a/b and AR interaction is independent of the promoter context. The likelihood that this synergy was due to the presence of AREs or Stat5-binding sites on the Stat5-regulated cyclin D1 and β-casein promoters or MMTV and probasin promoters, respectively, was ruled out by verification searches using the P-Match pattern matrix and transcription-binding site search (38). Moreover, experiments in LNCaP cells showed coaction between endogenously expressed Stat5a/b and AR as well. When Stat5a/b and AR were cotransfected to both LNCaP cells and T47D human breast cancer cells, no synergic interaction of Stat5a/b and AR was observed in T47D human breast cancer cells versus LNCaP cells. This suggests the transcriptional coaction between Stat5a/b and AR is specific for prostate cancer cells or it may be specific for androgen-regulated cells in general. The enhancement of transcriptional activity of liganded AR by Stat5a/b in reporter gene assays was equal to or stronger than what has previously been reported for promotion of AR by Stat3, Akt, or mitogen-activated protein kinase signaling pathways (39–43). Importantly, the functional synergy between AR and Stat5a/b was reflected in protein expression levels of the AR target gene PSA and a Stat5a/b target gene cyclin D1, further suggesting biological significance of Stat5a/b interaction with AR in prostate cancer cells. It is possible that prostate cancers with activated Stat5a/b have higher PSA expression as a surrogate of active AR, which is an interesting question to address in a future study. Limitations of the work presented here include exclusive use of plasmid reporter gene assays. Therefore, future studies using gene expression arrays need to determine the extent of transcriptional synergy between Stat5 and AR in prostate cancer cells *in vitro* and *in vivo*.

The precise details underlying the synergy between active Stat5a/b and AR signaling in prostate cancer cells remain to be elucidated. We currently favor a model where functional synergy between Stat5a/b and AR may involve shared nuclear translocation mechanisms between the two. This hypothesis is supported by the findings of increased nuclear accumulation of ligand-induced AR in cells with an active Stat5 signaling pathway, whereas liganded AR enhanced nuclear accumulation of active Stat5a/b in PC-3 cells expressing PrlR, Stat5a, and AR. Importantly, double immunostaining of AR and Stat5 with indirect fluorescence further supported the concept of active Stat5 and liganded AR enhancing nuclear localization of each other. Our results further show that active Stat5a/b and liganded AR physically complexed in prostate cancer cells, which was shown by coimmunoprecipitation of Stat5a/b and AR. This complex was shown in PC-3 cells cotransfected with Stat5a/b and AR, as well as in LNCaP cells that endogenously express Stat5a/b and AR. Stat proteins are transported to the nucleus by karyopherins (44). Provided that importin-α and importin-β are involved in nuclear import of both Stats (45) and AR (37) and that our results indicated physical interaction between active Stat5a/b and AR in coimmunoprecipitation experiments, it is possible that Stat5-AR protein complex involves karyopherin proteins. Finally, coexpression of active Stat5a with liganded AR led to enhanced binding of ligand-induced AR to DNA in AR EMSA analysis. We propose that enhanced DNA-binding of AR is due to higher abundance of AR in the nuclei when the Stat5a/b signaling pathway is active simultaneously with AR signaling in prostate cancer cells. Alternatively, the stability of DNA binding of AR may be increased by the presence of active Stat5 in the nuclei. Future studies using Chip assays need to determine whether Stat5a/b and AR stay in a complex on AR or Stat5-regulated promoters in prostate cancer cells. The fluorescence immunostaining of Stat5 and AR revealed that liganded AR induced nuclear translocation of Stat5 in the absence of Prl stimulation. At the same time, Prl-activated Stat5 induced nuclear translocation of unliganded AR in prostate cancer cells. The function and importance of the nonphosphorylated Stat5a/b or unliganded AR brought into the nuclei by liganded AR or phosphorylated Stat5a/b, respectively, remain to be determined. Interestingly, direct DNA binding and transcriptional regulation of certain promoters by unphosphorylated Stat monomers have been shown previously (46). We have shown that Stat5a/b is constitutively active in human prostate cancer cells (12, 22). It is possible that this pool of constitutively phosphorylated Stat5 dimers in prostate cancer cells translocate to the nucleus complexed with liganded AR in the absence of exogenous Prl stimulation.

Stat5a/b is in the active state in 95% of hormone-refractory recurrent human prostate cancers. In addition, the likelihood of Stat5a/b being active in primary human prostate cancer was higher ($P = 0.02$) if the patient had been treated with androgen deprivation as an adjuvant therapy before radical prostatectomy. It is currently unclear whether increased frequency of Stat5a/b activation in primary prostate cancer followed by adjuvant hormone therapy reflects the effect of androgen ablation on prostate cancer cells or rather a selection of tumor cells with progressive features. The finding of a mutually cooperative interaction between active Stat5a/b and AR in prostate cancer cells may have relevance for growth of prostate cancer during androgen deprivation in the presence of low levels of circulating androgens. This is because the components required for the interaction of both these two prostate growth promoting signaling pathways are present in

hormone-independent prostate cancers. Similarly to active Stat5a/b, AR expression persists in prostate cancer despite the progression to hormone-refractory state (30, 47). The effects of the synergy between Stat5a/b and AR signaling on the growth of prostate tumors *in vivo* will be crucial for the understanding of the full biological significance of Stat5-AR interaction. In addition, it will be important to determine whether Stat5a/b and AR transcriptionally synergize on AR-driven and Stat5a/b-driven transcription when AR is liganded by AR ligands that are present during clinical androgen ablation therapy, such as antiandrogens or adrenal androgens.

The molecular mechanisms underlying constitutive activation of Stat5a/b in hormone-refractory human prostate cancer are currently unclear. Such mechanisms may involve autocrine Prl (12, 13, 21). Our previous results showed that autocrine Prl expression in prostate cells was associated with high-grade prostate cancer (12). Moreover, we have also shown that Jak2 is the predominant kinase that activates Stat5a/b in prostate cancer cells (12), and activating mutations of Jak2 have been recently described in hematopoietic malignancies resulting in constitutive activation of Stat5 (48). Such Jak2 mutations may also occur in advanced prostate cancer. A third potential mechanism for constitutive activation of Stat5a/b in prostate cancer is amplification of Stat5a/b genes. This is a subject worthwhile of a study because Stat5a/b genes are located on chromosome 17 (49), which is frequently altered in prostate cancer (50).

In summary, the findings presented in this work show for the first time transcriptional synergy between AR and Stat5 signaling in prostate cancer. This finding is important because Stat5a/b and AR are transcription factors that inhibit apoptosis and promote growth of prostate cancer cells. Ongoing work aims to determine the extent of transcriptional synergy between Stat5a/b and AR on Stat5a/b-driven and AR-driven gene transcription in prostate cancer, as well as the molecular mechanisms underlying the coaction between Stat5a/b and AR. Future studies will also establish the effect of Stat5a/b-AR synergy on prostate tumor growth *in vivo*. Finally, identification of small molecule inhibitors for Prl-Jak2-Stat5 signaling pathway may be explored as a new strategy combined with androgen deprivation for therapy of hormone-refractory prostate cancer.

Acknowledgments

Received 8/3/2007; revised 9/14/2007; accepted 10/30/2007.

Grant support: American Cancer Society grant RSG-04-196-01-MGO, Department of Defense Prostate Cancer grants W81XWH-05-01-0062 and W81XWH-07-01-0411, and NIH National Cancer Institute grant 1RO1CA113580-01A1. This project was funded, in part, under a grant with the Pennsylvania Department of Health (the Department specifically disclaims responsibility for any analyses, interpretations, or conclusions). Shared resources of Kimmel Cancer Center are partially supported by NIH Cancer Center Support grant CA56036-08.

The costs of publication of this article were defrayed in part by the payment of page charges. This article must therefore be hereby marked *advertisement* in accordance with 18 U.S.C. Section 1734 solely to indicate this fact.

We thank Dr. Hallgeir Rui for Ad-WT-PrlR construct, Dr. Mary Vore for the sodium taurocholate cotransporting protein–luciferase construct, Dr. Munkhtsegtseg Dorj for help in immunostainings, Jacqueline Lutz for critical reading of the manuscript, and Drs. Chenguang Wang and Richard Pestell for providing the cyclin D1 promoter–luciferase construct.

References

1. Isaacs JT, Isaacs WB. Androgen receptor outwits prostate cancer drugs. Nat Med 2004;10:26–7.
2. Gelmann EP. Molecular biology of the androgen receptor. J Clin Oncol 2002;20:3001–15.
3. Mangelsdorf DJ, Thummel C, Beato M, et al. The nuclear receptor superfamily: the second decade. Cell 1995;83:835–9.
4. Koivisto P, Kononen J, Palmberg C, et al. Androgen receptor gene amplification: a possible molecular mechanism for androgen deprivation therapy failure in prostate cancer. Cancer Res 1997;57:314–9.
5. Heinlein CA, Chang C. Androgen receptor in prostate cancer. Endocr Rev 2004;25:276–308.
6. Buchanan G, Yang M, Harris JM, et al. Mutations at the boundary of the hinge and ligand binding domain of the androgen receptor confer increased transactivation function. Mol Endocrinol 2001;15:46–56.
7. Ihle JN. The Stat family in cytokine signaling. Curr Opin Cell Biol 2001;13:211–7.
8. Rui H, Djeu JY, Evans GA, Kelly PA, Farrar WL. Prolactin receptor triggering. Evidence for rapid tyrosine kinase activation. J Biol Chem 1992;267:24076–81.
9. Rui H, Lebrun JJ, Kirken RA, Kelly PA, Farrar WL. JAK2 activation and cell proliferation induced by antibody-mediated prolactin receptor dimerization. Endocrinology 1994;135:1299–306.
10. Nevalainen MT, Ahonen TJ, Yamashita H, et al. Epithelial defect in prostates of Stat5a-null mice. Lab Invest 2000;80:993–1006.
11. Ahonen TJ, Harkonen PL, Rui H, Nevalainen MT. PRL signal transduction in the epithelial compartment of rat prostate maintained as long-term organ cultures *in vitro*. Endocrinology 2002;143:228–38.
12. Li H, Ahonen TJ, Alanen K, et al. Activation of signal transducer and activator of transcription 5 in human prostate cancer is associated with high histological grade. Cancer Res 2004;64:4774–82.
13. Nevalainen MT, Valve EM, Ingleton PM, Nurmi M, Martikainen PM, Harkonen PL. Prolactin and prolactin receptors are expressed and functioning in human prostate. J Clin Invest 1997;99:618–27.
14. Nevalainen MT, Valve EM, Makela SI, Blauer M, Tuohimaa PJ, Harkonen PL. Estrogen and prolactin regulation of rat dorsal and lateral prostate in organ culture. Endocrinology 1991;129:612–22.
15. Ahonen TJ, Harkonen PL, Laine J, Rui H, Martikainen PM, Nevalainen MT. Prolactin is a survival factor for androgen-deprived rat dorsal and lateral prostate epithelium in organ culture. Endocrinology 1999;140:5412–21.
16. Wennbo H, Kindblom J, Isaksson OG, Tornell J. Transgenic mice overexpressing the prolactin gene develop dramatic enlargement of the prostate gland. Endocrinology 1997;138:4410–5.
17. Kindblom J, Dillner K, Ling C, Tornell J, Wennbo H. Progressive prostate hyperplasia in adult prolactin transgenic mice is not dependent on elevated serum androgen levels. Prostate 2002;53:24–33.
18. Kindblom J, Dillner K, Sahlin L, et al. Prostate hyperplasia in a transgenic mouse with prostate-specific expression of prolactin. Endocrinology 2003;144:2269–78.
19. Steger RW, Chandrashekar V, Zhao W, Bartke A, Horseman ND. Neuroendocrine and reproductive functions in male mice with targeted disruption of the prolactin gene. Endocrinology 1998;139:3691–5.
20. Nevalainen MT, Valve EM, Ingleton PM, Harkonen PL. Expression and hormone regulation of prolactin receptors in rat dorsal and lateral prostate. Endocrinology 1996;137:3078–88.
21. Nevalainen MT, Valve EM, Ahonen T, Yagi A, Paranko J, Harkonen PL. Androgen-dependent expression of prolactin in rat prostate epithelium *in vivo* and in organ culture. FASEB J 1997;11:1297–307.
22. Ahonen TJ, Xie J, LeBaron MJ, et al. Inhibition of transcription factor Stat5 induces cell death of human prostate cancer cells. J Biol Chem 2003;278:27287–92.
23. Kazansky AV, Spencer DM, Greenberg NM. Activation of signal transducer and activator of transcription 5 is required for progression of autochthonous prostate cancer: evidence from the transgenic adenocarcinoma of the mouse prostate system. Cancer Res 2003;63:8757–62.
24. Li H, Zhang Y, Glass A, et al. Activation of signal transducer and activator of transcription-5 in prostate cancer predicts early recurrence. Clin Cancer Res 2005;11:5863–8.
25. Zhang Y, Glass A, Bennett N, Oyama KA, Gehan E, Gelmann EP. Long-term outcomes after radical prostatectomy performed in a community-based health maintenance organization. Cancer 2004;100:300–7.
26. Saramaki O, Willi N, Bratt O, et al. Amplification of EIF3S3 gene is associated with advanced stage in prostate cancer. Am J Pathol 2001;159:2089–94.
27. Nevalainen MT, Xie J, Torhorst J, et al. Signal transducer and activator of transcription-5 activation and breast cancer prognosis. J Clin Oncol 2004;22:2053–60.
28. Nevalainen MT, Xie J, Bubendorf L, Wagner KU, Rui H. Basal activation of transcription factor signal transducer and activator of transcription (Stat5) in nonpregnant mouse and human breast epithelium. Mol Endocrinol 2002;16:1108–24.
29. Behbod F, Nagy ZS, Stepkowski SM, et al. Specific inhibition of Stat5a/b promotes apoptosis of IL-2-responsive primary and tumor-derived lymphoid cells. J Immunol 2003;171:3919–27.
30. Trachtenberg J, Walsh PC. Correlation of prostatic nuclear androgen receptor content with duration of response and survival following hormonal therapy in advanced prostatic cancer. J Urol 1982;127:466–71.
31. Ganguly TC, O'Brien ML, Karpen SJ, Hyde JF, Suchy FJ, Vore M. Regulation of the rat liver sodium-dependent bile acid cotransporter gene by prolactin. Mediation of transcriptional activation by Stat5. J Clin Invest 1997;99:2906–14.
32. Matsumura I, Kitamura T, Wakao H, et al. Transcriptional regulation of the cyclin D1 promoter by STAT5: its involvement in cytokine-dependent growth of hematopoietic cells. EMBO J 1999;18:1367–77.
33. Gouilleux F, Wakao H, Mundt M, Groner B. Prolactin induces phosphorylation of Tyr694 of Stat5 (MGF), a

prerequisite for DNA binding and induction of transcription. EMBO J 1994;13:4361–9.
34. Ku CY, Loose-Mitchell DS, Sanborn BM. Both Sertoli and peritubular cells respond to androgens with increased expression of an androgen response element reporter. Biol Reprod 1994;51:319–26.
35. Kasper S, Rennie PS, Bruchovsky N, et al. Cooperative binding of androgen receptors to two DNA sequences is required for androgen induction of the probasin gene. J Biol Chem 1994;269:31763–9.
36. Gregory CW, He B, Wilson EM. The putative androgen receptor-A form results from *in vitro* proteolysis. J Mol Endocrinol 2001;27:309–19.
37. Black BE, Paschal BM. Intranuclear organization and function of the androgen receptor. Trends Endocrinol Metab 2004;15:411–7.
38. Chekmenev DS, Haid C, Kel AE. P-Match: transcription factor binding site search by combining patterns and weight matrices. Nucleic Acids Res 2005; 33:W432–7.
39. Lin D-L, Keller ET. Mechanism of interleukin-6 promotion of androgen receptor function in prostate cancer cells. Iowa City: International Conference on Prostate Cancer Research; 1999.
40. Abreu-Martin MT, Chari A, Palladino AA, Craft NA, Sawyers CL. Mitogen-activated protein kinase kinase kinase 1 activates androgen receptor-dependent transcription and apoptosis in prostate cancer. Mol Cell Biol 1999;19:5143–54.
41. Yeh S, Lin HK, Kang HY, Thin TH, Lin MF, Chang C. From HER2/Neu signal cascade to androgen receptor and its coactivators: a novel pathway by induction of androgen target genes through MAP kinase in prostate cancer cells. Proc Natl Acad Sci U S A 1999;96:5458–63.
42. Ueda T, Bruchovsky N, Sadar MD. Activation of the androgen receptor N-terminal domain by interleukin-6 via MAPK and STAT3 signal transduction pathways. J Biol Chem 2002;277:7076–85.
43. Chen T, Wang LH, Farrar WL. Interleukin 6 activates androgen receptor-mediated gene expression through a signal transducer and activator of transcription 3-dependent pathway in LNCaP prostate cancer cells. Cancer Res 2000;60:2132–5.
44. Sekimoto T, Imamoto N, Nakajima K, Hirano T, Yoneda Y. Extracellular signal-dependent nuclear import of Stat1 is mediated by nuclear pore-targeting complex formation with NPI-1, but not Rch1. EMBO J 1997;16:7067–77.
45. McBride KM, Banninger G, McDonald C, Reich NC. Regulated nuclear import of the STAT1 transcription factor by direct binding of importin-α. EMBO J 2002;21: 1754–63.
46. Chatterjee-Kishore M, Wright KL, Ting JP, Stark GR. How Stat1 mediates constitutive gene expression: a complex of unphosphorylated Stat1 and IRF1 supports transcription of the LMP2 gene. EMBO J 2000;19: 4111–22.
47. Sadi MV, Walsh PC, Barrack ER. Immunohistochemical study of androgen receptors in metastatic prostate cancer. Comparison of receptor content and response to hormonal therapy. Cancer 1991;67: 3057–64.
48. Baxter EJ, Scott LM, Campbell PJ, et al. Acquired mutation of the tyrosine kinase JAK2 in human myeloproliferative disorders. Lancet 2005;365:1054–61.
49. Clark J, Edwards S, Feber A, et al. Genome-wide screening for complete genetic loss in prostate cancer by comparative hybridization onto cDNA microarrays. Oncogene 2003;22:1247–52.
50. Gillanders EM, Xu J, Chang BL, et al. Combined genome-wide scan for prostate cancer susceptibility genes. J Natl Cancer Inst 2004;96:1240–7.